Experimental investigation of a highly efficient, low-cost PVC-Rollers Sandwich (PVC-RS) seismic isolation

Author(s):
Tsiavos, Anastasios; Sextos, Anastasios; Stavridis, Andreas; Dietz, Matt; Dihoru, Luiza; Alexander, Nicholas A.

Publication date:
2021-10

Permanent link:
https://doi.org/10.3929/ethz-b-000488153

Originally published in:
Structures 33, https://doi.org/10.1016/j.istruc.2021.05.040

Structures 33 (2021) 1590–1602

Contents lists available at ScienceDirect

Structures

journal homepage: www.elsevier.com/locate/structures

Experimental investigation of a highly efficient, low-cost PVC-Rollers Sandwich (PVC-RS) seismic isolation

Anastasios Tsiavos [a,*], Anastasios Sextos [b], Andreas Stavridis [c], Matt Dietz [d], Luiza Dihoru [d], Nicholas A. Alexander [e]

[a] Lecturer, Department of Civil, Environmental and Geomatic Engineering, ETH Zurich, Switzerland
[b] Professor in Earthquake Engineering and Head of Earthquake and Geotechnical Engineering Research Group, Department of Civil Engineering, University of Bristol, UK
[c] Associate Professor, Department of Civil, Structural and Environmental Engineering, University at Buffalo, United States
[d] Research Fellow, Department of Civil Engineering, University of Bristol, UK
[e] Associate Professor in Structural Dynamics, Department of Civil Engineering, University of Bristol, UK

ARTICLE INFO

Keywords:
PVC-Rollers Sandwich
Roller bearings
Low-cost seismic isolation
Shaking table tests

ABSTRACT

This paper focuses on the large-scale experimental investigation of a novel, highly efficient, low-cost and easily constructible seismic isolation system, defined as PVC-Rollers Sandwich (PVC-RS) seismic isolation. The proposed system is based on the placement of spherical roller bearings between two PVC surfaces in a sandwich configuration. This configuration triggers a desirable rolling behaviour between the rollers and the PVC surfaces, thus isolating the motion of the structure from the ground excitation. The large-scale shaking table investigation of the seismic response of a scaled-down masonry and a scaled-down steel model of a seismically isolated prototype structure using PVC-RS has unveiled the activation of the rolling behaviour of the structure at a desirably low acceleration amplitude of 0.05g-0.1g. The reliability of this low-acceleration response of the structure was confirmed for ground motion excitations of different amplitudes and frequency characteristics. The experimentally tested variation on the amount, the material and the diameter of the roller bearings allows for the implementation of different design alternatives of the presented system, according to the seismic design requirements and the seismic performance objectives for each location.

1. Introduction

Seismic isolation is a response modification strategy aiming at the decoupling of the response of buildings and bridges from the motion of the ground during an earthquake excitation and thus the protection of these structures from seismic damage. Subsequently, the design of an efficient seismic isolation system is inextricably linked with the determination of an energy dissipation mechanism which triggers this decoupling behaviour at a reasonably low peak ground acceleration.

The engineering concept of seismic energy dissipation through the inclusion of a thin granular layer between selected structural members was utilized for the first time many centuries ago. Greek and Roman temples, Chinese and Japanese Pagodas [1] and Persian monuments, such as the Tomb of Cyrus [2] were constructed by blocks designed to slide against each other during an earthquake ground motion excitation.

During the last decades, the decoupling behaviour of several highly engineered seismic isolation devices [3,4] has been analytically [5–7] and experimentally [8–12] investigated. These investigations have led to the design and development of a wide range of efficient seismic isolation systems, which have been applied in many developed countries worldwide. However, the highly engineered processes required for the construction of these systems and the necessity for the construction of an additional slab designed to transmit the seismic load uniformly to the seismic isolation devices make these systems resource- and cost-demanding compared to conventional structures. Subsequently, a large amount of conventional structures worldwide are designed to maintain their seismic response in the elastic range with a strength reduction factor q=1, as a means of engineering a zero-earthquake-damage design solution. However, the elastic design of structures increases significantly the construction cost of these structures.

In light of these limitations, the extension of the application of seismic isolation to a broader range of structures and countries

* Corresponding author at: Department of Civil, Environmental and Geomatic Engineering (D-BAUG), ETH Zurich, HIL E14.2, Stefano-Franscini-Platz 5, 8093 Zurich, Switzerland.
E-mail address: tsiavos@ibk.baug.ethz.ch (A. Tsiavos).

https://doi.org/10.1016/j.istruc.2021.05.040
Received 9 July 2020; Received in revised form 3 April 2021; Accepted 16 May 2021
Available online 26 May 2021

necessitates the development of easily constructible and cost-effective seismic isolation solutions. The aim of this study is to propose an innovative, highly efficient, low-cost seismic isolation system that is easily constructible and applicable to a large number of countries worldwide. This system can lay the basis for a low-cost design alternative to the elastic design of structures with q=1.

Several researchers have explored a potential cost reduction of the current seismic isolation techniques by using materials that can be easily resourced or recycled. Tsang et al. [13] and Tsiavos et al. [14] have investigated the use of a sand-rubber foundation layer consisting of recycled rubber below structures as a low-cost sliding seismic isolation strategy for developing countries. A similar soil-based sliding system was experimentally investigated by Banovic et al. [15], while Nanda et al. [16] explored the frictional characteristics of marble and geosynthetics. The use of recycled rubber as a low-cost seismic isolation was extended to unbonded fiber reinforced elastomeric isolators by Spizzuoco et al. [17], Habieb et al. [18,19], Toopchi-Nezhad et al. [20] and Ping et al. [21]. The influence of the isolation degree on the seismic reliability and life-cycle costs of a seismically isolated structure was investigated by Castaldo et al. [22]. Yegian and Katakal [23] and Yegian and Katan [24] proposed the use of smooth synthetic liners below the foundation of a structure or between soil layers as a sliding seismic energy dissipation mechanism. Tsiavos et al. [25,26] proposed a novel PVC 'sand-wich' (PVC-s) sliding seismic isolation for developing countries, comprising a thin layer of sand, which is sandwiched between two PVC surfaces.

Albeit important focus has been made on the investigation of sliding low-cost seismic isolation strategies, a commensurate depth of research has not been invested on the dynamics of rolling as a means of low-cost seismic isolation of structures.

The mechanics of sliding-rolling behavior between various elements and interfaces has been widely investigated and utilised for the seismic protection of structures in the past. Coulomb [27] demonstrated that the frictional resistance of a rolling wheel is proportional to the vertical load acting on the wheel, and inversely proportional to the radius of the wheel. The attractively low frictional values obtained during the rolling motion of steel hard spheres over rubber surfaces have been first illuminated by Tabor [28] and Eldredge and Tabor [29]. Greenwood et al. [30] shed light into the exact mechanism that triggers the rolling motion of these spheres by attributing this low rolling resistance to significant hysteresis losses due to the deformation of rubber.

The aforementioned attractive frictional characteristics attributed to the rolling motion of spherical bearings have been utilized on the investigation and design of several highly manufactured rolling-based seismic isolation systems. The evolution of the application of these mechanisms to seismic isolation of structures was summarized by Harvey and Kelly [31]. Chung et al. [32] developed an analytical model elucidating the efficiency of rolling energy dissipation mechanisms for seismic isolation of structures. Tsai et al. [33] conducted shaking table tests on the seismic behaviour of isolated bridges using steel rolling seismic isolation devices. A similar seismic isolation system using steel spheres rolling over rubber sheets has been experimentally validated by Harvey et al. [34]. Cilsalar and Constantinou [35] illuminated the reliability of rolling seismic isolation systems compared to the existing sliding systems due to their independence from hysteretic or frictional heating when proposing a novel rolling seismic isolation system based on urethane spherical seismic isolators with a steel core. Foti and Kelly [36], Foti et al. [37] and Foti [38] have introduced and experimentally investigated a seismic isolation concept based on the rolling of steel cylinders between two rubber surfaces, utilizing the favourable rolling mechanics on the interface of these materials examined by Tabor [28]. These favourable rolling characteristics on the steel-rubber interface were analytically substantiated by Menga et al. [39].

Nevertheless, the existing efficient, yet highly manufactured, rolling seismic isolation technologies do not integrate the beneficial rolling characteristics of the individual elements and interfaces in a low-cost and easily constructible seismic isolation system.

Along these lines, the aim of this study is the experimental large-scale shaking table investigation of a highly efficient, low-cost and easily constructible seismic isolation. The investigated seismic isolation, defined as PVC-Rollers Sandwich, comprises a sandwich configuration based on the rolling of spherical bearings, sandwiched between two PVC surfaces. The dynamic response of two different three times-scaled down seismically isolated structures is investigated at the shaking table of University of Bristol: A steel model structure and a masonry model structure. The two different model structures are subjected to unidirectional and threedimensional earthquake ground motion excitation of different amplitudes. This investigation provides a comprehensive basis for further investigations in the future towards the development of a highly efficient, low-cost and easily constructible seismic isolation strategy.

2. Seismic isolation of the prototype structure

A prototype structure corresponding to a low-rise masonry structure designed using the PVC-Rollers Sandwich seismic isolation system is presented in Fig. 1.

The prototype 4 m×6 m masonry structure consists of four 25 cm thick masonry walls, based on a 20 cm thick concrete slab. A light roof is supported by the four 2.5 m tall masonry walls as a means of engineering a low mass at the top of the structure, leading to a minimum seismic demand.

The proposed PVC-Rollers Sandwich (PVC-RS) configuration is presented in Fig. 1: A predetermined amount of spherical roller bearings is sandwiched between two 6 mm thick PVC sheets. The roller bearings are roughly uniformly distributed on the surface of the bottom PVC sheet. The upper PVC surface is placed on the top of the distributed roller bearings. The concrete slab can be either casted on the upper PVC surface using lateral restraints during the casting process or pre-casted in connection with the PVC sheet and then placed on the top of the distributed roller bearings. The use of steel or borosilicate glass roller bearings is proposed in this study due to their low cost and availability in a wide range of countries worldwide. The two different roller bearing types are presented in Fig. 2. The diameter of the steel roller bearings used in this study is 6 mm, while the corresponding diameter for glass ballotini bearings is 2.5 mm.

The construction process related to the implementation of the PVC-RS seismic isolation system on the prototype structure is the following: A 20 cm deep excavation is performed first to enable the placement of a 15 cm thick hardcore layer as a rigid base and a 5 cm thick sand layer below the bottom PVC surface of the PVC-RS configuration. The importance of the placement of the 5 cm thick sand layer below the structure is dual: First, the increase of the reliability of the seismic isolation system, due to the addition of a second, pure-sliding seismic isolation mechanism which could be activated at a PGA = 0.3 g according to Tsiavos et al. [25,26]. This sliding mechanism can be activated between the bottom PVC sheet and the sand layer in case the first PVC-RS rolling mechanism is not activated. Second, the mobilization of a PVC-sand sliding isolation mechanism can be designed to inhibit a potential excessive rolling-sliding displacement due to the activation of the low-friction PVC-RS mechanism. The restraining force in this case would emerge from the higher friction coefficient between PVC and sand (approximately 0.3) compared to the low-friction characterizing the PVC-roller interface. An additional restraining mechanism consisting of a 20 cm thick, 30 degrees inclined gravel layer placed above the surrounding soil at a distance of 100 cm from the foundation boundaries is designed to impede excessive rolling or sliding displacements of the structure. A polythene membrane is placed between the sand layer and the hardcore layer to prevent any exchange of material between the sand layer and the surrounding soil.

The use of two alternative seismic isolation mechanisms, a rolling isolation between the upper PVC surface and the sandwiched rollers and

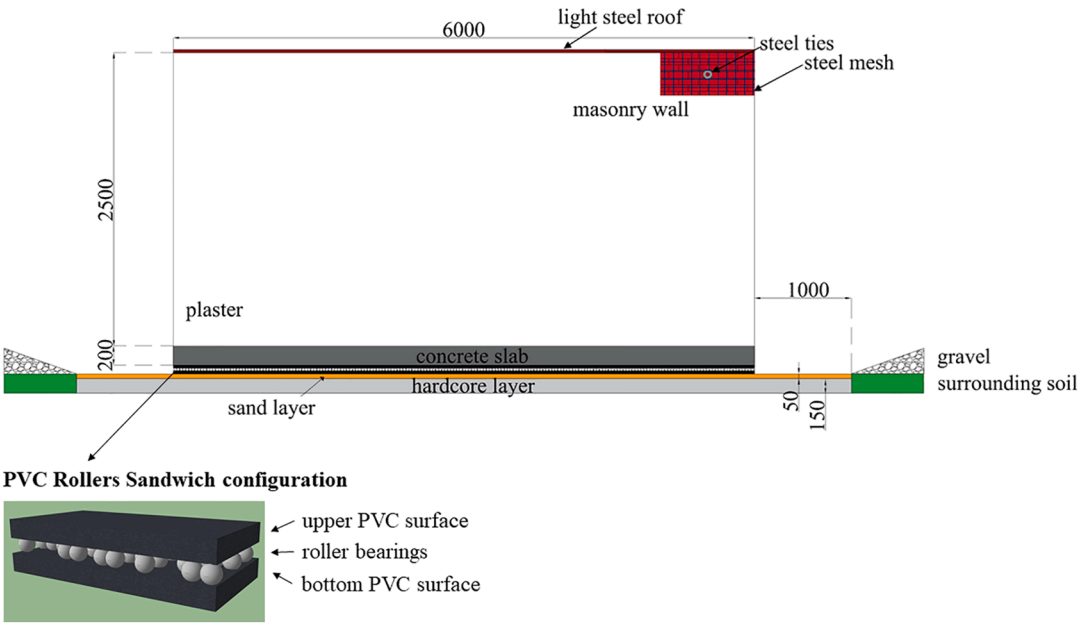

Fig. 1. Application of the low-cost PVC-RS seismic isolation approach to a prototype structure.

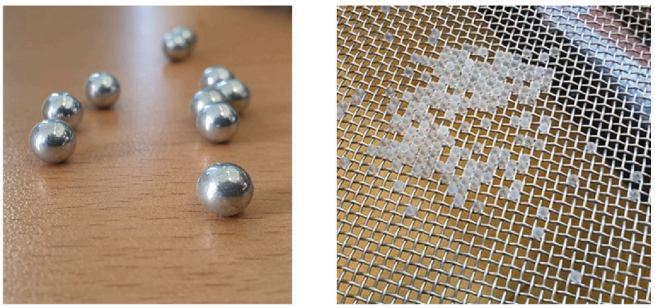

Fig. 2. (a) Steel and (b) glass ballotini bearings used for the PVC-RS seismic isolation proposed in this study.

a sliding isolation between the bottom PVC surface and the sand foundation layer are not the only seismic protection mechanisms proposed in this study. The addition of steel ties, each fixed on the outer sides of two opposite masonry walls of the structure and the attachment of a steel mesh to both sides of each wall of the structure are additional seismic protection mechanisms aimed at the seismic protection of masonry structures below the earthquake intensity level, at which the seismic isolation mechanisms are activated. Both protection mechanisms are selected to prevent the structure from an out-of-plane failure, which is a commonly observed source of seismic damage in masonry structures. The placement of a light roof on the top of the structure and the use of high-strength mortar between the brick joints are additional seismic protection mechanisms focusing on the decrease of the seismic mass (and seismic demand) and the increase of the shear resistance (and seismic capacity) of the masonry structure, respectively.

3. Experimental setup

3.1. Design and construction of the experimental setup

The experimental setup, shown in Fig. 3, comprises the large-scale investigation of a scaled-down 2.3tons masonry model of the prototype structure at the shaking table of University of Bristol. The horizontal dimensions of the structure are three times scaled-down compared to the prototype structure. The height of the model structure is 1 m.

The size of the clay bricks used for the construction of the model structure is 10 cm×6 cm×21.5 cm and the thickness of the cement mortar joints is 1 cm. These dimensions follow at 1:1 scale the brick sizes and mortar thicknesses of the prototype structure, chosen to simulate common practices in the construction of low-cost masonry structures. The cement to sand ratio value used for the cement mortar is 1:4, leading to an experimentally determined compression strength value of $f_{c,\ mortar} = 6.6$ MPa. This strength value was obtained through compression tests of mortar prisms conducted at University of Bristol.

A reinforced concrete slab with a thickness of 20 cm was designed to facilitate the foundation of the masonry model structure and its crane transportation to and from the shaking table through lifting anchors during the experimental investigation.

The constructed masonry model structure characterized by the aforementioned mechanical and geometrical properties is based on a 20 cm thick reinforced concrete slab. The PVC-Rollers sandwich configuration presented in Fig. 1 is implemented in the model structure using one upper 2mx1.3 m, 6 mm thick PVC sheet, 2000 sandwiched steel roller bearings with a diameter of 6 mm weighing 1.2 kg and two bottom 2 m×1.3 m, 6 mm thick PVC sheets, positioned symmetrically along the centroid of the bottom slab. The tensile strength of the PVC material at yield is 55Mpa, while its modulus of elasticity is 3100 MPa. The ball indentation hardness of the surface of the PVC sheet is 82 MPa. The roller bearing surface density with respect to the area of the upper PVC surface that is projected on the bottom PVC surface is 800 rollers/m^2. This surface density value corresponds to a low fraction (2.5%) of the maximum roller surface density of 32,000 rollers/m^2, which can be theoretically achieved by the rollers of this diameter. The upper PVC surface is attached to the bottom of the concrete slab, thus emulating the connection of the two materials after the casting of the concrete slab on the PVC-based, permanent formwork.

A 3 m×3 m, 5 cm thick sand layer with properties shown on Table 1 was placed below the bottom PVC surface as a foundation layer intended to create the desirable performance objectives discussed in the design of the prototype structure. The thickness of the layer was selected to minimize potential soil-structure interaction effects [40], which could inhibit the sliding-rolling response of the structure. The deposition of the

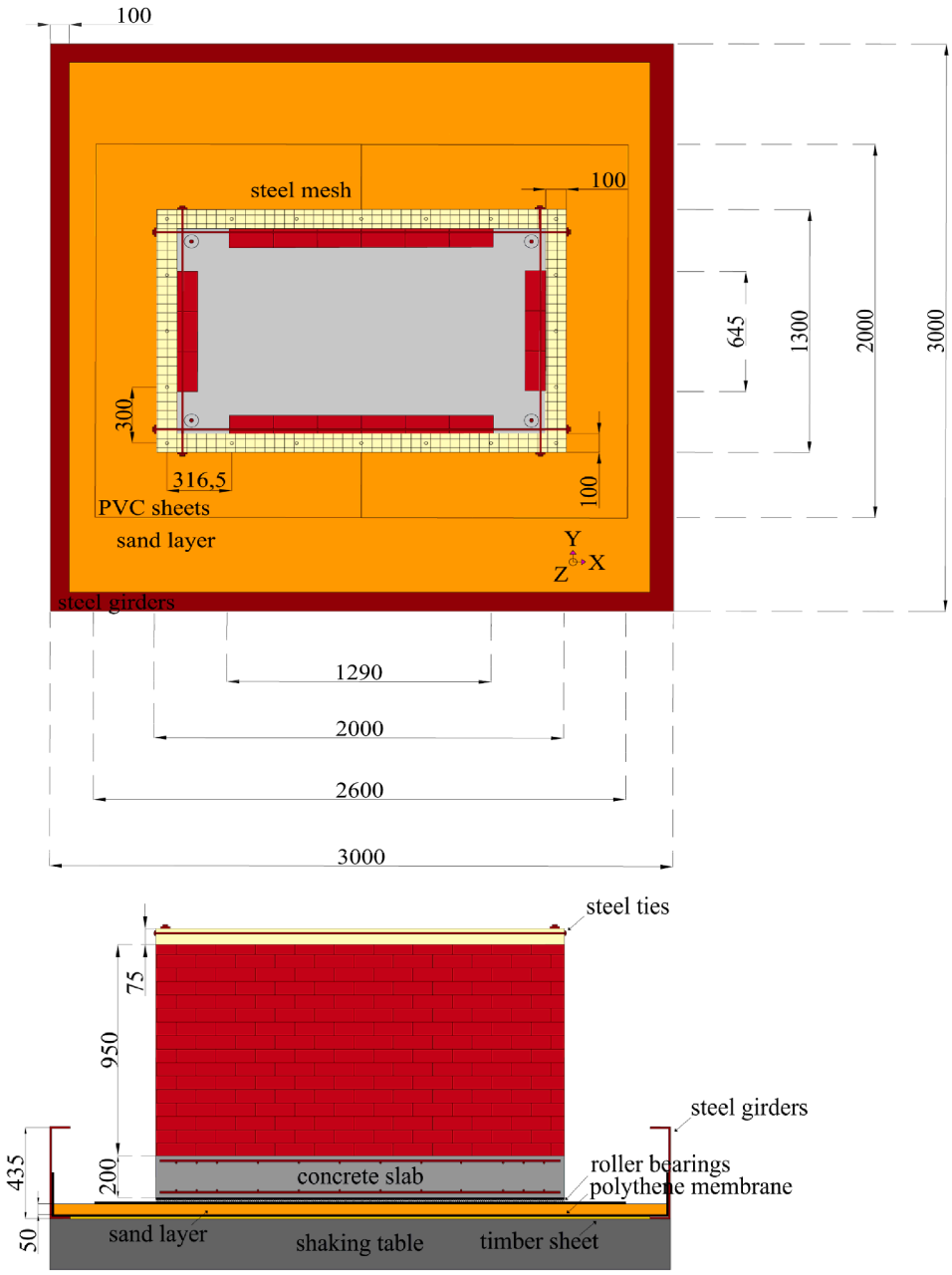

Fig. 3. Overview and side view of the designed experimental setup.

Table 1
Properties of the Leighton Buzzard 14–25 sand used in this study.

Specific gravity G_s	Void ratio e_{max}	Void ratio e_{min}	Mean size D_{50} (mm)	$C_u = D_{60}/D_{10}$	$C_g = D_{30}^2/D_{60}D_{10}$
2.65	0.84	0.53	0.883	1.439	0.996

sand was performed with zero-height drop, thus creating an experimentally derived sand density value of 1580 kg/m^3. Four C-shaped girders are fixed on the edges of the shaking table and a polythene membrane is placed between the girders and the sand layer to facilitate the formation of a box below the structure, capable of preventing any leakage of material during the shaking table excitation.

The deposition of steel roller bearings above the bottom PVC layer of the constructed experimental setup is shown in Fig. 4. The steel roller bearings are placed with a zero-height drop on the bottom PVC layer, thus impeding the potential rolling of the steel bearings out of the boundaries defined by the desirable contact surface between the concrete slab and the bottom PVC layer. Emphasis is given on the achievement of the maximum possible uniformity in the deposition of the steel bearings below the structure. This deposition aims at creating a uniform distribution of the vertical loading and stresses on the steel roller bearings, which is optimal for the activation of the rolling resistance of the bearings at the lowest rolling friction coefficient [28–30].

A steel wire mesh with a grid of 50 mm×50 mm and four steel ties with a diameter of 6 mm were attached to the structure, implementing the additional seismic protection mechanisms proposed in this study. A timber ring beam is mechanically attached to the top course of the bricks to allow the fixation of four steel ties as lateral restraints against the out-of-plane failure of the walls. A gypsum coating is used as a plastering layer above the steel mesh to create a uniform contact between the steel mesh and the wall, while a light white paint is used as the external coating layer on the walls of the constructed structure, shown in Fig. 5.

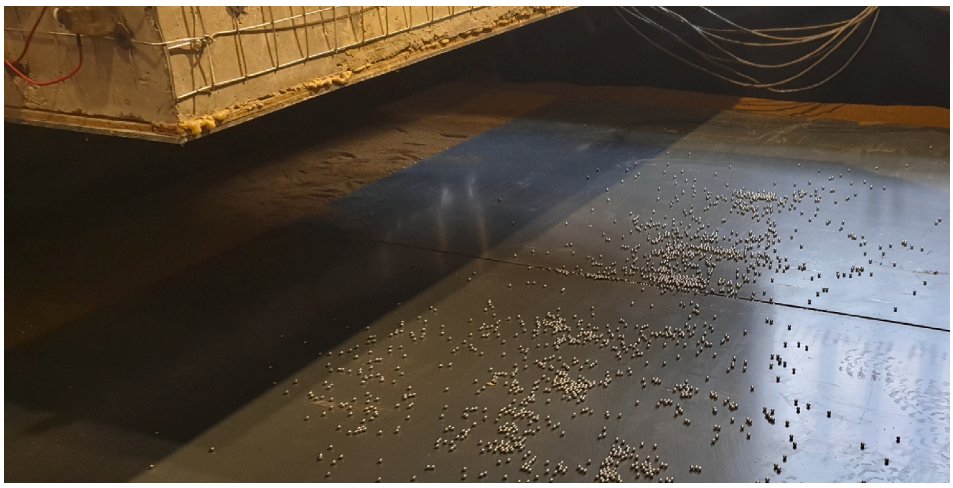

Fig. 4. Deposition of steel roller bearings on the bottom PVC surface.

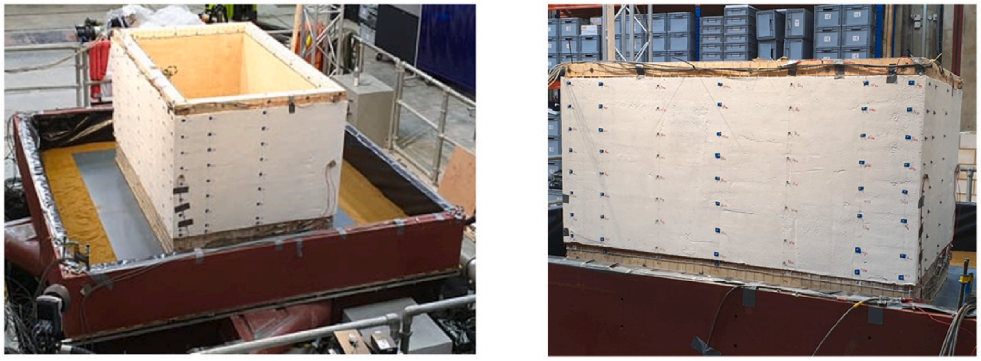

Fig. 5. (a) Overview and (b) Side view of the constructed experimental setup.

3.2. Instrumentation

The attachment of 27 uniaxial accelerometers and 100 displacement markers to the walls of the experimentally investigated model structure facilitates the continuous monitoring of the acceleration and the displacement time history response of the structure during the shaking table motion. Three infrared cameras are used to track the movement of the applied displacement markers in three directions, thus allowing the capturing of the three-dimensional motion of the structure. The applied instrumentation and the corresponding instrumentation plan are shown in Figs. 5 and 6, respectively.

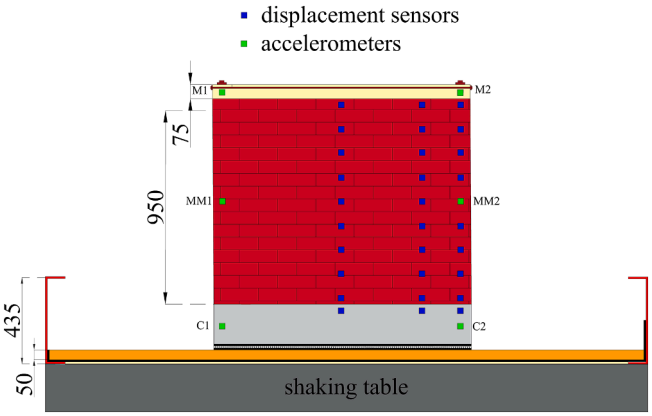

Fig. 6. Side view of the instrumentation plan.

3.3. Dimensional analysis

The extrapolation of the results obtained from a ground motion excitation of a scaled-down model to the prototype structure requires the conduction of dimensional analysis. This study has determined three dimensionless ratios, shown on Table 2, which should be maintained between the model and the prototype structure to facilitate the similitude in the obtained results: First, the dimensionless strength ratio $\Pi_1=\mu g/\text{PGA}$ (μ being the static friction coefficient and g the acceleration of gravity) expresses the strength of the rolling-sliding interface with respect to the Peak Ground Acceleration. The equality between the friction coefficient μ obtained for the model structure and the prototype is satisfied through the design of the model structure to be subjected to the same vertical foundation stress $\sigma'_v = 9$ kPa with the prototype.

Table 2
Dimensionless ratios and design parameters used in the dimensional analysis.

Dimensionless ratios	Similitude (Prototype to model)	Design parameters	Similitude (Prototype to model)
$\Pi_1 = \mu g/\text{PGA}$	1:1	Length L [m]	1:3
$\Pi_2 = T_y^{\sim}/T_g$	1:1	Fixed-base period T_y [s]	1:1
$\Pi_3 = t/\text{h}$	1:1	Vertical stress σ'_v [kPa]	1:1

Therefore, the strength ratio Π_1 is maintained between the model and the prototype structure, subjected to ground motions of a predetermined Peak Ground Acceleration. Second, the vibration period ratio $\Pi_2 = T_{\tilde{y}}/T_g$, determining the relation between the flexible-base period $T_{\tilde{y}}$ of the structure over the predominant period of the excitation T_g, defined as the period where the 5% velocity spectrum attains its maximum [41]. The model structure has been designed to have the same fixed-base period $T_y = 0.1$ s with the prototype structure. The conduction of white-noise tests with amplitude $A = 0.05$g and vibration frequency range $f =$ 0–100 Hz in the direction of the applied ground motion excitation has shown that the corresponding flexible-base period of the structure $T_{\tilde{y}} = 0.125$ s is close with the fixed-base value. Hence, the vibration period ratio Π_2 is preserved between the model and the prototype structure, subjected to ground motions of a predetermined predominant period T_g. Third, the dimensionless ratio $\Pi_3 = t/h$ expressing the thickness of the walls t over their height h in the model and the prototype structure. The construction of the walls of the model structure with a thickness t = 10 cm and height $h = 100$ cm satisfies the preservation of this ratio $\Pi_3 = 0.1$, with respect to the prototype structure with walls of a thickness t = 25 cm and height $h = 250$ cm.

3.4. Testing protocol

The testing protocol of the dynamic investigation of the seismic response of the presented model structure consist of four different amplitudes of the Chi-Chi 1999 recorded ground motion excitation, obtained from the PEER strong ground motion database [42]. This ground motion record was selected as a ground motion record, characterized by a broad frequency content. The response spectrum of the ground motion record is rich in both the short and the high frequency range and can be viewed in the study of Tsiavos et al. [25,26]. The scaling of the recorded motion to four different Peak Ground Acceleration levels: 0.2 g, 0.4 g, 0.6 g and 0.8 g allows the determination of the response of the isolated structure to different earthquake intensity and hazard levels. The characteristics of the applied scaled ground motion ensemble are shown on Table 3. All the presented motions have been applied in the Y-Direction of the experimental setup shown in Figs. 3, 5 using the 6-DOF shaking table of University of Bristol.

4. Shaking table investigation of the response of a seismically isolated masonry structure

The presented masonry model structure is first excited by the Chi-Chi 1999 ground motion excitation with an amplitude of 0.2 g (No. 1 on Table 3). The applied shaking table motion is shown in Fig. 7.

The effect of the uniformity in the distribution and the corresponding vertical pressure on the steel roller bearings with a diameter of 6 mm is illustrated through the comparison of the response of the structure for two different roller bearing surface density values: A surface density of 200 rollers/m^2 corresponding to stress concentration and non-uniform pressure on the steel rollers and a surface density of 800 rollers/m^2 corresponding to a more uniform pressure on the steel roller bearings.

Table 3
Testing protocol of recorded earthquake ground motions used for the excitation of the masonry structure (PEER NGA Database, 2018 [42]).

No.	Date	Earthquake and Site	M_w	R (km)	Component	Scaled PGA (g)
1	21/9/1999	Chi-Chi, CHY080	7.6	2.69	CHY080-E	0.2
2	21/9/1999	Chi-Chi, CHY080	7.6	2.69	CHY080-E	0.4
3	21/9/1999	Chi-Chi, CHY080	7.6	2.69	CHY080-E	0.6
4	21/9/1999	Chi-Chi, CHY080	7.6	2.69	CHY080-E	0.8

The acceleration time history response recorded on the top of the structure is presented in Fig. 7. As shown in the figure, the maximum acceleration of the structure in the case of uniform pressure on the bearings is 0.05 g, corresponding to a reduction ratio $R = 0.2$ g/0.05 g = 4 with respect to the Peak Ground Acceleration of the applied ground motion. However, the corresponding maximum acceleration response of the structure isolated with a smaller amount of steel roller bearings with non-uniform vertical pressure is the same with the applied ground motion, namely 0.2 g. The difference in the response of the two different roller bearing configurations is attributed to the activation of a rolling seismic isolation mechanism for the steel rollers under uniform pressure, which remains inactive in the case of stress concentration on the steel rollers. The attachment of steel ties and steel mesh on the investigated masonry structure enabled its seismic protection for the case of 200 rollers/m^2 (Fig. 7), in which the seismic isolation was not activated. This rolling displacement (relative to the shaking table motion) reaches a maximum of 12 cm for the uniformly pressed rollers, as shown in Fig. 8. The corresponding displacement of the structure isolated with unequally loaded rollers relative to the shaking table motion is zero, thus confirming the absence of observed rolling response for this roller configuration at this seismic intensity level.

The excitation of the structure by the same ground motion, scaled at a higher intensity level of 0.4 g (No. 2 on Table 3) confirmed the trends shown for the amplitude of 0.2 g: The maximum acceleration of the structure isolated with uniformly loaded rollers, shown in Fig. 9, was 0.05 g, thus reducing the ground motion acceleration to a reduction ratio of $R = 0.4$ g/0.05 = 8. The corresponding maximum acceleration for a non-uniform pressure on the rollers was approximately 0.2 g, leading to a reduction ratio of $R = 0.4$ g/0.2 g = 2 compared to the applied motion. However, the activation of a rolling isolation system at a higher acceleration level (0.2 g) for the non-unifromly loaded rollers is not necessarily unfavorable: It can lead to the design of a more horizontally stable structure, which is more resistant to the action of wind forces. The presentation of a variety of experimentally derived responses of the presented seismic isolation system aims at providing different design alternatives, thus offering a desirable freedom to the civil engineering community to decide on the optimal configuration of the proposed system. This decision should be based on the geometry of the isolated structure, its performance objectives, the seismic hazard level and the wind excitation on the location.

The activation of the rolling behaviour of the uniformly loaded steel rollers at a lower level of friction compared to the non-uniform loading of the rollers is demonstrated in Fig. 10: The uniformly pressed rollers manifest rolling at the 9th second of the motion, reaching a maximum displacement of 15 cm and a residual displacement of 12 cm. In contrast, the rolling displacement of the unequally loaded rollers relative to the shaking table is triggered on the 18th second of the motion (Fig. 10b), leading to a maximum displacement of 10 cm and a residual displacement of 7 cm. The remarkable sliding displacement of seismically isolated structures subjected to long-period seismic excitation has been observed by Ordonez et al. [43], Castaldo and Tubaldi [44], Tsiavos et al. [45–47] and Tsiavos and Stojadinovic [48].

The initiation of sliding when the applied ground motion acceleration exceeds the value of 0.05 g for the uniformly loaded rollers is consistently and systematically presented through the sudden increase of the horizontal rolling displacement of the structure (relative to the motion of the shaking table) at this acceleration level shown in Figs. 8, 10 and 12.

The effectiveness of the proposed seismic isolation system for the case of the masonry structure (Fig. 3) isolated with steel roller bearings (Fig. 2a) and subjected to two of the ground motion records presented in this study (No 1, 2 as shown in Table 3) is summarized through the use of the acceleration reduction ratio $R = \text{PGA}/\max|a_{sb}|$. The values of this ratio, defined by the Peak Ground Acceleration over the maximum of the acceleration of the isolated structure a_{sb} (sliding base) are summarized for different ground motion records and different surface densities of

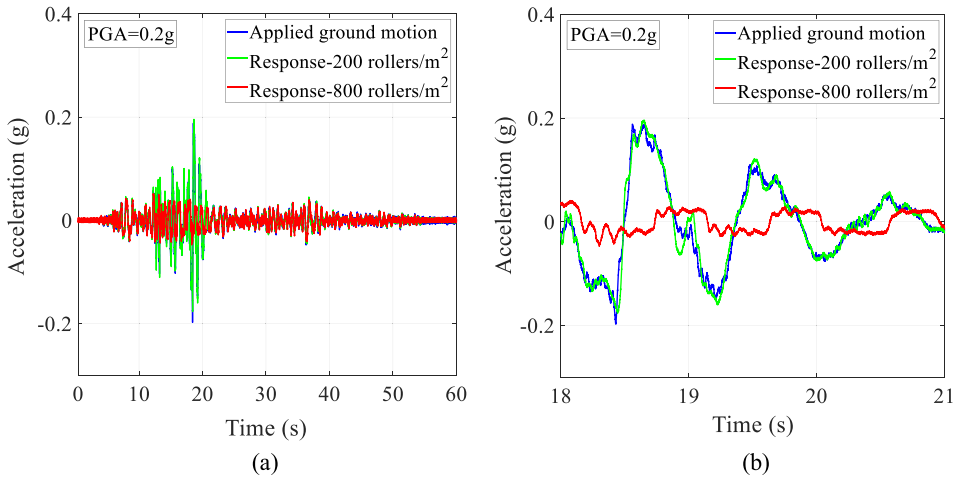

Fig. 7. (a) Full and (b) enlarged acceleration time history response on the top of the masonry structure (mean value of M1, M2 in Fig. 6) due to the applied Chi-Chi 1999 recorded ground motion excitation with PGA = 0.2 g (No. 1 on Table 3) for varying roller surface density values.

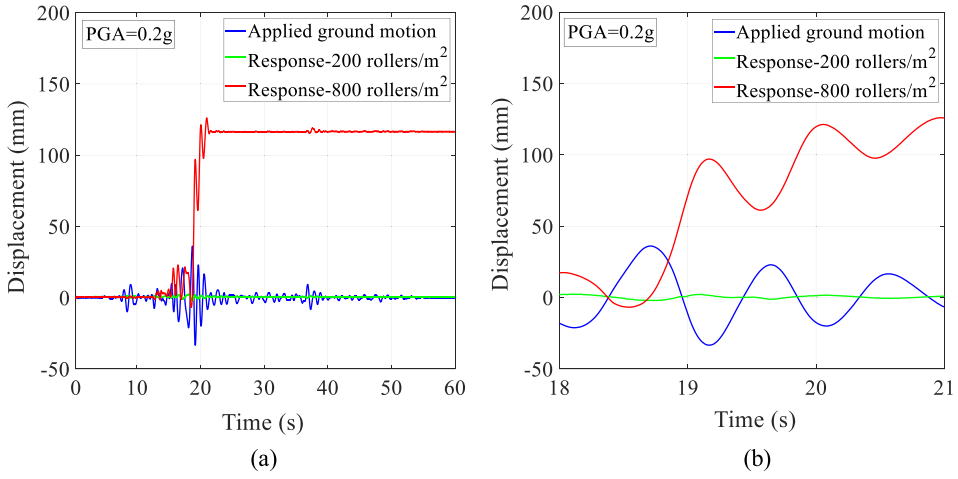

Fig. 8. (a) Full and (b) enlarged rolling horizontal displacement time history response of the masonry structure (relative to the shaking table motion) due to the applied Chi-Chi 1999 recorded ground motion excitation with PGA = 0.2 g (No. 1 on Table 3) for varying roller surface density values.

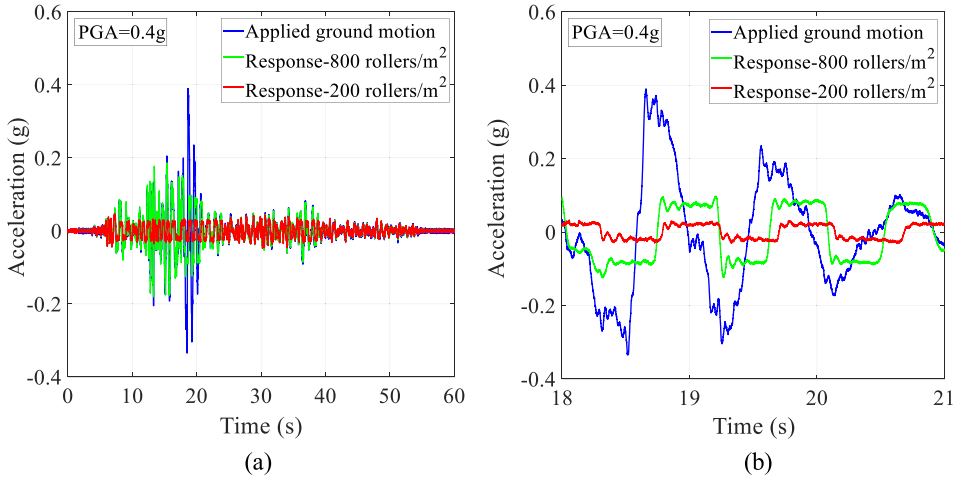

Fig. 9. (a) Full and (b) enlarged acceleration time history response on the top of the masonry structure (mean value of M1, M2 in Fig. 6) due to the applied Chi-Chi 1999 recorded ground motion excitation with PGA = 0.4 g (No. 2 on Table 3) for varying roller surface density values.

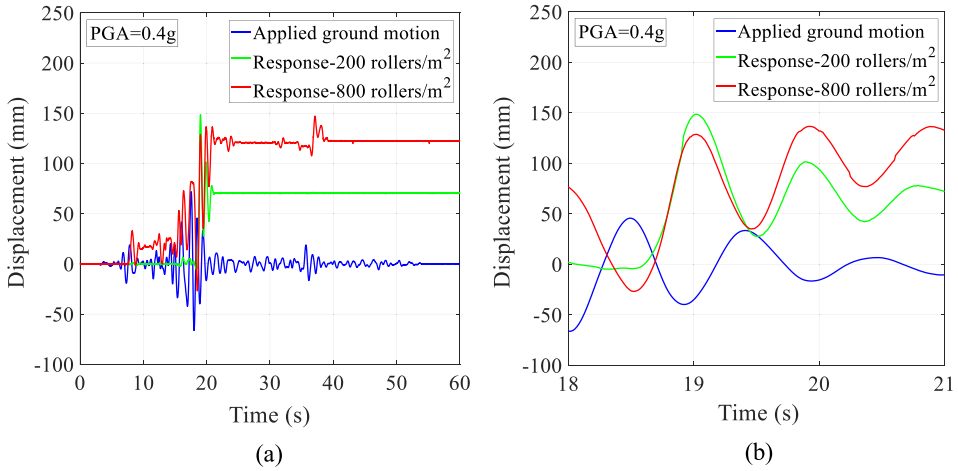

Fig. 10. (a) Full and (b) enlarged rolling horizontal displacement time history response of the masonry structure (relative to the shaking table motion) due to the applied Chi-Chi 1999 recorded ground motion excitation with PGA = 0.4 g (No. 2 on Table 3) for varying roller surface density values.

Table 4
Values of the acceleration reduction ratio R for different ground motion records and different surface densities of rollers/m^2 (Ground motion ensemble shown in Table 3).

Ground motion No.	Number of rollers/ m^2	PGA (g)	max$\lvert a_{sb}\rvert$ (g)	R = PGA/max$\lvert a_{sb}\rvert$
1	200 rollers/m^2	0.4	0.2	2
2	200 rollers/m^2	0.6	0.2	3
1	800 rollers/m^2	0.4	0.05	8
2	800 rollers/m^2	0.6	0.05	12

rollers/m^2 in the following Table 4:

As shown in the Table, the use of the proposed seismic isolation system can reduce the seismic acceleration (and consequently the seismic force) acting on the structure from 2 times ($R = 2$ for 200 rollers/m^2) up to 12 times (R = 12 for 800 rollers/m^2) relative to the Peak Ground Acceleration.

Interestingly, the initiation of rolling of the non-uniformly distributed bearings is not always related to lower sliding displacement. Figs. 11 and 12 elucidate the acceleration and rolling displacement response of the structure, excited by a ground motion acceleration amplitude of 0.6 g (No 3 on Table 3). The sequence of the scaled pulse components of the motion is such, that the continuous rolling behaviour of the uniformly loaded low-friction roller bearings shown in Fig. 12 leads to a lower maximum displacement (23 cm) compared to the non-uniform loading case, which manifests an instantaneous displacement of 25 cm during the PGA of 0.6 g. Nevertheless, the acceleration reduction ratio for the two systems is R = 0.6 g/0.05 g = 12 for the uniformly loaded bearings and R = 0.6 g/0.2 g = 3 for the non-uniformly loaded case. The plastic deformation on the PVC surface due to the stress concentration above the steel roller bearings during the sliding-rolling movement of the non-uniformly loaded rollers is shown in Fig. 13.

5. Shaking table investigation of the response of a seismically isolated steel structure

5.1. Influence of the aspect ratio and the mass distribution of the structure

The quantification of the influence of the aspect ratio, the material of the structure and the distribution of its weight on the seismic performance of the proposed seismic isolation system are of paramount importance for the determination of the efficiency of the system. Hence, a steel structure was designed to have the same weight with the masonry structure (2.3 tons) and was fixed on the same 20 cm thick concrete slab, founded on the proposed PVC-RS isolation system. However, the mass of the structure in this case is concentrated on a steel slab, fixed at a height of 0.53 m above the foundation level. The constructed experimental setup is shown in Fig. 14.

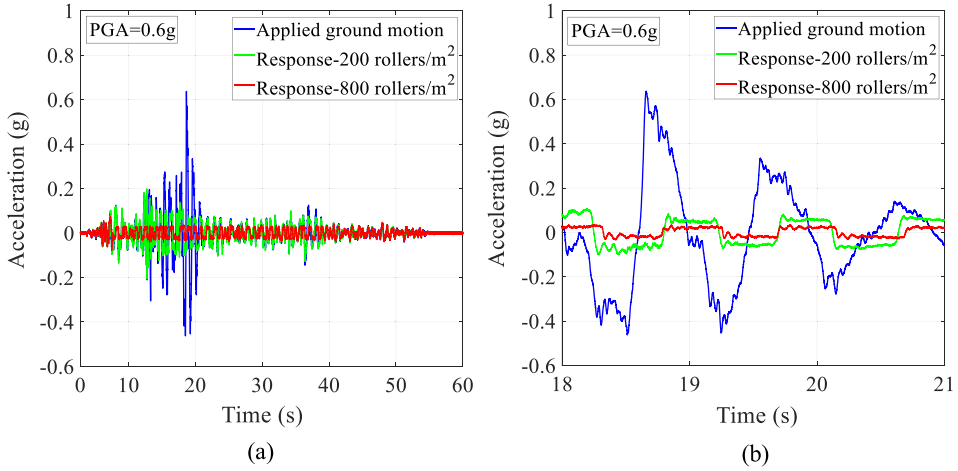

Fig. 11. (a) Full and (b) enlarged acceleration time history response on the top of the masonry structure (mean value of M1, M2 in Fig. 6) due to the applied Chi-Chi 1999 recorded ground motion excitation with PGA = 0.6 g (No. 2 on Table 3) for varying roller surface density values.

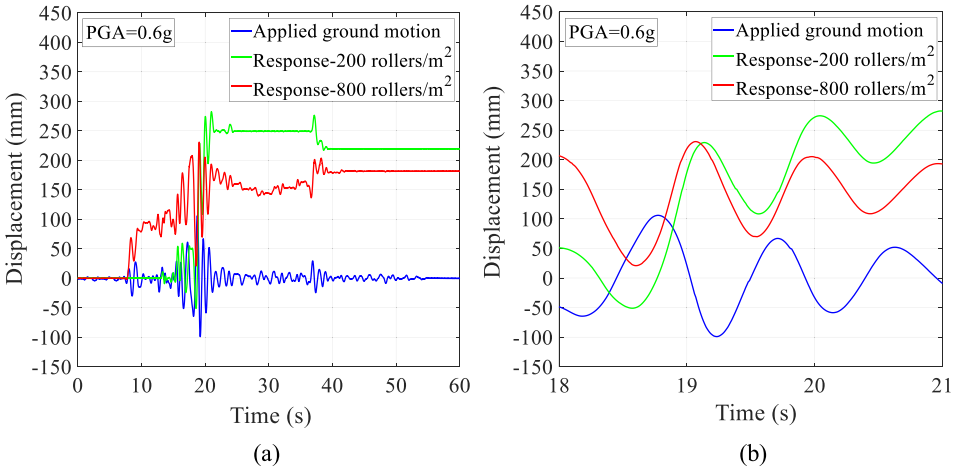

Fig. 12. (a) Full and (b) enlarged rolling horizontal displacement time history response of the masonry structure (relative to the shaking table motion) due to the applied Chi-Chi 1999 recorded ground motion excitation with PGA = 0.6 g (No. 2 on Table 3) for varying roller surface density values.

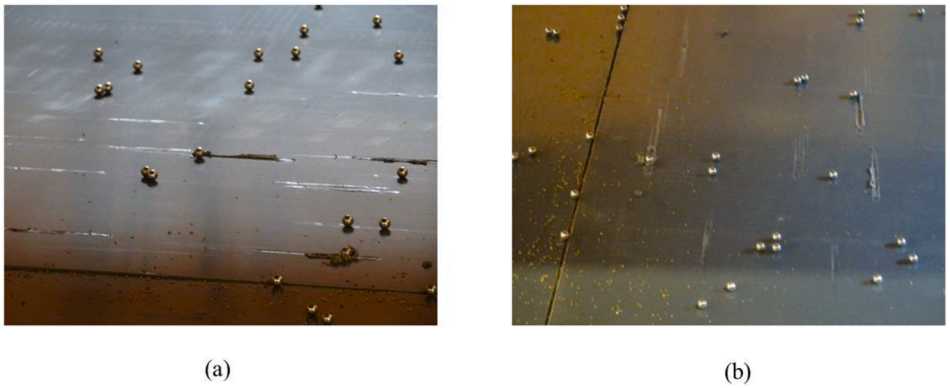

Fig. 13. (a) Side view and (b) top view of the sliding-rolling displacement of the non-uniformly loaded bearings due to stress concentration.

Fig. 14. Side view of the constructed experimental setup.

The presented setup allows for the investigation of the response of a steel structure with a substantially different aspect ratio (H/B = 0.6 m/2m = 0.3) and mass distribution compared to the previously investigated masonry structure (H/B = 1 m/1.3 m = 0.76), when the ground motion excitation is applied in X-Direction of the experimental setup. The instrumentation plan and the direction of shaking for this setup are shown in Fig. 15.

The instrumentation of the experimental setup presented in Fig. 15 entails 25 accelerometers and 16 displacement markers, which are tracked by 5 high-speed cameras. The ground motion ensemble

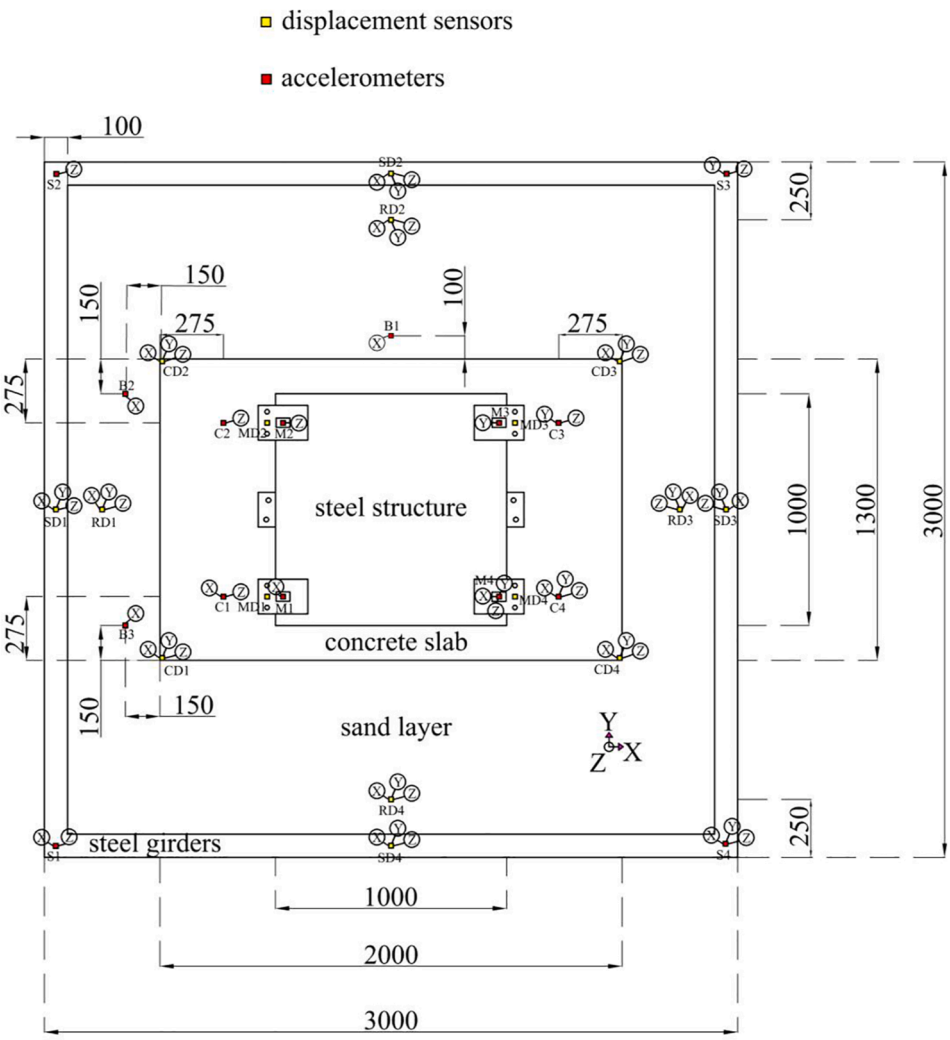

Fig. 15. Instrumentation plan.

Table 5
Testing protocol of recorded earthquake ground motions used for the excitation of the steel structure (PEER NGA Database, 2018 [42]).

No.	Date	Earthquake and Site	M_w	R (km)	Component	Scaled PGA (g)
1	21/9/1999	Chi-Chi, CHY080	7.6	2.69	CHY080-E	0.2
2	21/9/1999	Chi-Chi, CHY080	7.6	2.69	CHY080-E	0.4
3	21/9/1999	Chi-Chi, CHY080	7.6	2.69	CHY080-E	0.6
4	21/9/1999	Chi-Chi, CHY080	7.6	2.69	CHY080-E	0.8
5	6/4/2009	L'Aquila, Parking	6.3	5.38	LAQ-AM043XTE	0.2
6	6/4/2009	L'Aquila, Parking	6.3	5.38	LAQ-AM043XTE	0.4

presented for the masonry structure was extended by two additional, three-directional motions, recorded during the L'Aquila 2009 earthquake. The scaled ground motion ensemble presented on Table 5 was applied in the X-Direction of the experimental setup (Fig. 15). The design of this steel structure for a foundation vertical stress $\sigma'_v = 9$ kPa and a fixed-base vibration period $T_x = 0.1$ s satisfies the similitude and the preservation of the dimensionless ratios Π_1, Π_2 between the model and the prototype structure presented in the dimensional analysis of the model structure.

Fig. 16 illuminates the comparison of the response of the steel structure presented in Fig. 14 with the masonry structure shown in Fig. 5 for a Chi-Chi 1999 ground motion excitation, scaled at an amplitude of 0.4 g (No 2 in Tables 3 and 5). Both structures were seismically isolated with the proposed PVC-RS isolation system, using steel rollers with a diameter of 6 mm and surface density of 800 rollers/m^2.

As shown in Fig. 16, the steel structure exhibited a slightly higher static friction coefficient of 0.1 before the initiation of the sliding-rolling behaviour, compared to the corresponding value of 0.05 for the masonry structure. However, the kinetic friction value due to the rolling behaviour of the bearings during the maximum imposed ground acceleration (Fig. 16b) was exactly the same for the two structures. Therefore, the influence of the aspect ratio of the structure was limited to the initiation of the rolling-sliding behavior, leading to slightly higher static friction for structures of smaller aspect ratio and higher mass concentration on the top (Fig. 14).

5.2. *Steel roller bearings versus glass ballotini bearings*

The use of roller bearings for the design of the proposed PVC-RS seismic isolation system is not exhausted to steel roller bearings with a diameter of 6 mm. The effect of the material and the diameter of the roller bearings is demonstrated through the comparison of the response of the steel structure using two different roller types on the proposed

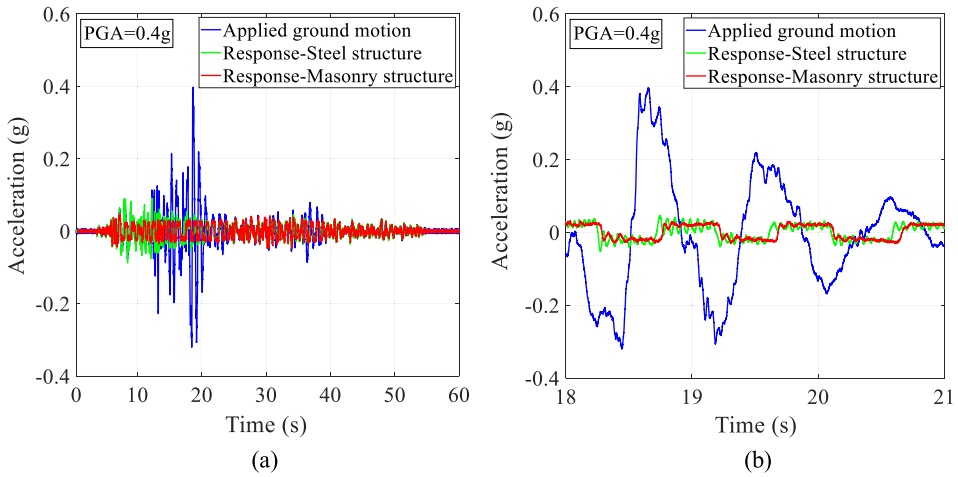

Fig. 16. (a) Full and (b) enlarged acceleration time history response on the top of the steel and the masonry structure (mean value of M1, M2 in Figs. 6, 15) due to the applied Chi-Chi 1999 recorded ground motion excitation with PGA = 0.4 g (No. 2 on Table 5).

isolation system (Fig. 2): Steel roller bearings with a diameter of 6 mm and surface density of 800 rollers/m^2 and glass ballotini bearings with a diameter of 2.5 mm and the same surface density. The acceleration response of the structure isolated with the two roller types for a PGA = 0.4 g is shown in Fig. 17.

As presented in Fig. 17, the use of glass ballotini roller bearings as the rolling elements of the proposed PCS-RS seismic isolation system increased the rolling-sliding friction coefficient to 0.15, compared to the steel roller bearing value of 0.05. Nevertheless, the use of glass as a material that does not require regular protection from corrosion compared to steel is proposed in this study as a design alternative for countries and locations with high humidity or corrosive environment. The cost of both roller bearing types is comparable and significantly lower than the cost of the highly engineered sliding elements of the existing seismic isolation strategies.

5.3. Influence of ground motion characteristics-vertical ground motion component

The excitation of the presented steel structure by the three-dimensional L'Aquila 2009 ground motion allows for the investigation of the effect of the variation of the frequency content and the simultaneity of three ground motion components on the observed response. The presented steel structure is seismically isolated with steel roller bearings with a diameter of 6 mm and surface density of 800 rollers/m^2. As shown in Fig. 18, the simultaneous presence of two horizontal and one vertical component on the ground motion excitation did not change the friction coefficient (0.05) and the corresponding maximum acceleration of the structure (0.05 g), which were observed for the unidirectional Chi-Chi 1999 ground motion.

6. Conclusions

The large-scale shaking table investigation presented in this study unveiled the attractive frictional characteristics of an innovative, low-cost rolling energy dissipation system. This system is based on the inclusion of steel or glass roller bearings between two PVC sheets. This sandwich configuration allows the initiation of a rolling displacement of the bearings and dissipation of seismic energy at a friction coefficient varying between 0.05 and 0.2.

The presented seismic isolation system, defined as PVC-Rollers Sandwich (PVC-RS) seismic isolation is the fundamental component of an ensemble of low-cost engineering solutions that are proposed in this study for the seismic protection of masonry structures. The attachment of a steel mesh and steel ties, the use of a light roof and high-strength mortar are proposed as additional, low-cost engineering measures that could further increase the seismic resistance of masonry structures for earthquake intensities lower than the acceleration threshold for the

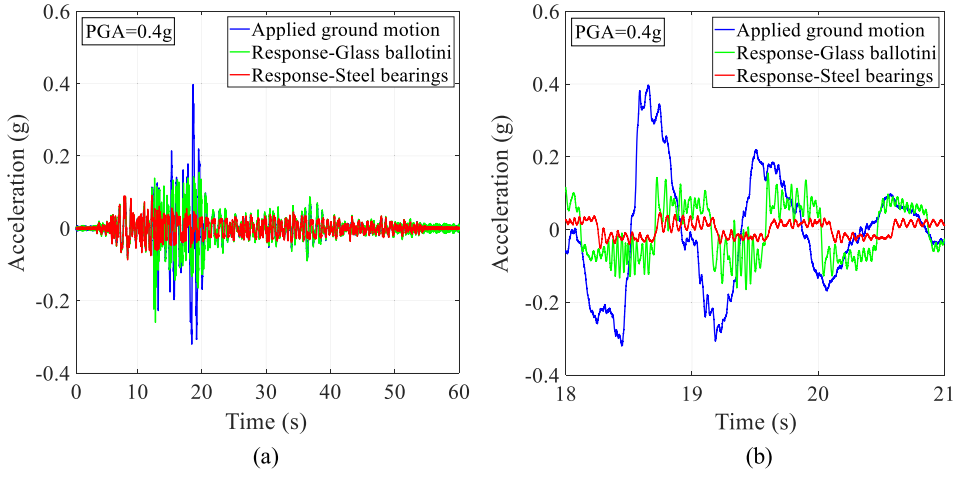

Fig. 17. (a) Full and (b) enlarged acceleration time history response on the top of the steel structure (mean value of M1, M2 in Fig. 15) due to the applied Chi-Chi 1999 recorded ground motion excitation with PGA = 0.4 g (No. 2 on Table 5) using two different roller bearing types.

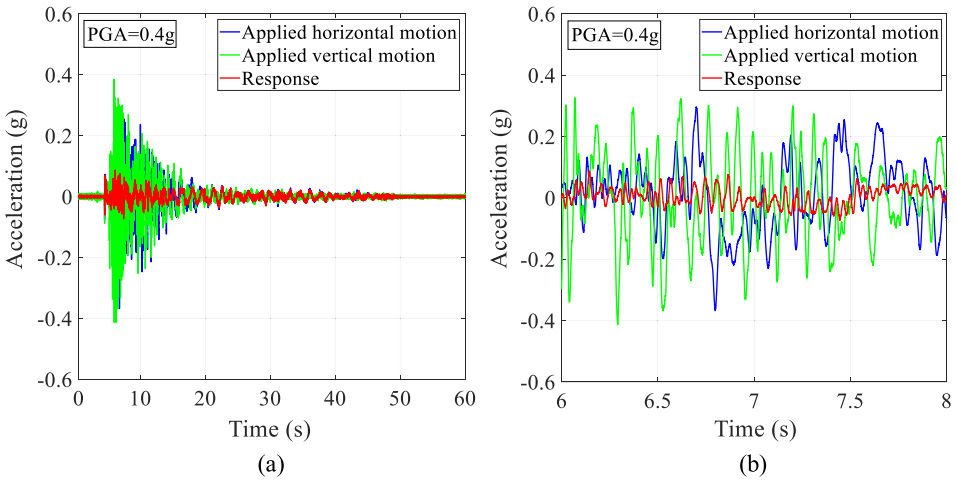

Fig. 18. (a) Full and (b) enlarged acceleration time history response on the top of the steel structure (mean value of M1, M2 in Fig. 15) due to the applied three-dimensional L'Aquila recorded ground motion excitation with PGA = 0.4 g (No. 6 on Table 5).

initiation of the rolling behaviour of the bearings.

A masonry and a steel structure, three-times scaled down models of the prototype structure were subjected to ground motions of different amplitudes and frequency characteristics. Both structures exhibited extensive rolling behaviour for a wide range of ground motion amplitudes. This behaviour was initiated approximately between acceleration amplitude levels of 0.05 and 0.1 g in case of uniformly distributed steel roller bearings of 6 mm diameter and surface density 800 rollers/m^2. The variation of the aspect ratio of the structure and the ground motion frequency characteristics did not affect significantly the rolling response of the structures. Interestingly, the obtained desirable acceleration response with a maximum at 0.1 g was maintained even for the excitation of the structure by three-dimensional motions with a strong vertical component.

The fundamental parameter that has been found to influence the rolling behaviour of the isolated model structures was the surface density of the roller bearings above the bottom PVC surface. The decrease of the density value from 800 rollers/m^2 to 200 rollers/m^2 has increased the obtained value of the static friction coefficient from 0.1 to 0.2. Not surprisingly, the use of a smaller amount of rollers increases the stress concentration above these rollers, thus inhibiting the initiation of rolling. The observed increase of the horizontal resistance of the structure for non-uniformly loaded roller bearings can be beneficial for the design of a more horizontally stable seismic isolation system, resistant to wind excitation.

A similar increase in the rolling friction coefficient has been observed during the replacement of the sandwiched steel roller bearings by glass ballotini bearings. The use of glass bearings can be advantageous in countries with highly corrosive environment, where the use of steel roller bearings is not recommended. At any case, special emphasis should be given in the protection of the steel bearings from corrosion through the use of protective paint or special protective coating layers.

The experimental investigation presented in this study elucidates the high efficiency of a PVC-rollers sandwich interface as an energy dissipation mechanism, which can be used as a low-cost component of a novel seismic isolation system. However, the presented energy dissipation mechanism leads to residual rolling displacement in the structure, reaching up to 20 cm for a ground motion excitation with a PGA = 0.6 g. The recentering of a structure, displaced at maximum by 20 cm from the original position after the occurrence of an earthquake event could be easily conducted through pulling by a truck.

Notwithstanding these limitations, the presentation of the use of different design alternatives by this study increases the flexibility in the application of the proposed isolation system to locations with different earthquake and wind hazard levels and different performance objectives. This flexibility, the low cost, the ease of construction and the high efficiency of the proposed seismic isolation system towards the reduction of the acceleration of the ground motion excitation show the potential of the application of the system as an effective protection of structures from seismic damage.

Declaration of Competing Interest

The authors declare that they have no known competing financial interests or personal relationships that could have appeared to influence the work reported in this paper.

Acknowledgements

This work is supported by the EPSRC-funded research project 'SAFER' (Seismic Safety and Resilience of Schools in Nepal, EP/P028926/1). Prof. George Mylonakis is gratefully acknowledged for his input on the dimensional analysis performed in this study. The authors would like to thank Dr. Adam Crewe for his recommendations on the design of the experimental setup. The technicians Mr. Dave Ward, Mr. Simon Ball, Mr. Mitchell Mictroy, the postdoctoral researcher Dr. Nicola Giordano and the students Mr. Yichen Zhang, Ms. Dominika Malkowska, Mr. Francesco Di Michele and Mr. Spyridon Diamantopoulos are kindly acknowledged for their technical assistance during the conduction of the presented large-scale experiments.

References

[1] Aicher S, Reinnhardt HW, Garrecht H. Materials and Joints in Timber Structures: Recent Developments of Technology. RILEM: Springer; 2014.
[2] Llunji M. Seismic Architecture: The architecture of earthquake resistant structures, MSPROJECT, 2016.
[3] Kelly JM. Aseismic base isolation: review and bibliography. Soil Dyn Earthquake Eng 1986;5(3):202–16.
[4] Buckle IG, Mayes RL. Seismic isolation history, application and performance—a world view. Earthquake Spectra 1990;6(2):161–201.
[5] Nagarajaiah S, Reinhorn AM, Constantinou MC. Nonlinear dynamic analysis of three-dimensional base isolated structures (3D-basis). National Center for Earthquake Engineering Research, State University of New York, Buffalo, Technical Report NCEER-89-0019, 1989.
[6] Siringoringo DM, Fujino Y. Seismic response analyses of an asymmetric base-isolated building during the 2011 Great East Japan (Tohoku) Earthquake. Struct Control Health Monitoring 2015;22(1):71–90. https://doi.org/10.1002/stc.1661.
[7] Fujino Y, Siringoringo DM. In: Seismic performance of an asymmetric base-isolated building in the 2011 Great East Japan Earthquake, Research and Applications in Structural Engineering, Mechanics and Computation. CRC Press; 2013. p. 137–8.
[8] Attary N, Symans M, Nagarajaiah S, Reinhorn AM, Constantinou MC, Sarlis AA, et al. Experimental shake table testing of an adaptive passive negative stiffness device within a highway bridge model. Earthquake Spectra 2015;31(4):2163–94.

[9] Mokha A, Constantinou MC, Reinhorn AM. Teflon bearings in base isolation. I: Testing. J Struct Eng (ASCE) 1990;116(2):438–54.
[10] Paulson TJ, Abrams DP, Mayes RL. Shaking-table study of base isolation for masonry buildings. J Struct Eng 1991;117(11):3315–36.
[11] Nikolic-Brzev S, Arya AS. Seismic isolation of masonry buildings-an experimental study. In: Proceedings of 11th World Conference on Earthquake Engineering 1996, Mexico City, Mexico. Elsevier, Abingdon, Paper No.1338.
[12] Mazza F, Mazza M, Vulcano A. Base-isolation systems for the seismic retrofitting of r.c. framed buildings with soft-storey subjected to near-fault earthquakes. Soil Dyn Earthquake Eng 2018;109:209–21.
[13] Tsang HH, Lam NTK, Yaghmaei-Sabegh S, Sheikh MN, Indraratna B. Geotechnical seismic isolation by scrap tire–soil mixtures. In: Proceedings of the 5th International Conference on Recent Advances in Geotechnical Earthquake Engineering and Soil Dynamics, San Diego, California, U.S., May 24–29, 2010.
[14] Tsiavos A, Alexander N, Diambra A, Ibraim E, Vardanega P, Gonzalez-Buelga A, et al. A sand-rubber deformable granular layer as a low-cost seismic isolation strategy in developing countries: experimental investigation. Soil Dyn Earthquake Eng 2019;125:105731.
[15] Banović I, Radnić J, Grgić N, Matešan D. The use of limestone sand for the seismic base isolation of structures. Adv Civ Eng 2018:9734283.
[16] Nanda RP, Agarwal P, Shrikhande M. Suitable friction sliding materials for base isolation of masonry buildings. J Shock Vibration 2012;19(6):1327–39.
[17] Spizzuoco M, Calabrese A, Serino G. Innovative low-cost recycled rubber-fiber reinforced isolator: experimental tests and finite element analyses. Eng Struct 2014;76:99–111.
[18] Habieb AB, Valente M, Milani G. Hybrid seismic base isolation of a historical masonry church using unbonded fiber reinforced elastomeric isolators and shape memory alloy wires. Eng Struct 2019;196:109281.
[19] Habieb AB, Valente M, Milani G. Implementation of a simple novel Abaqus user element to predict the behavior of unbonded fiber reinforced elastomeric isolators in macro-scale computations. Bull Earthq Eng 2019;17(5):2741–66.
[20] Toopchi-Nezhad H, Tait MJ, Drysdale RG. Shake table study on an ordinary low-rise building seismically isolated with SU-FREIs (stable unbonded-fiber reinforced elastomeric isolators). Earthquake Eng Struct Dyn 2009;38(11):1335–57.
[21] Tan P, Xu K, Wang B, Chang C, Liu H, Zhou F. Development and performance evaluation of an innovative low-cost seismic isolator. Sci China Technol Sci 2014;57(10):2050–61.
[22] Castaldo P, Palazzo B, Della VP. Life-cycle cost and seismic reliability analysis of 3D systems equipped with FPS for different isolation degrees. Eng Struct 2016;125:349–63.
[23] Yegian MK, Kadakal U. Foundation isolation for seismic protection using a smooth synthetic liner. J Geotechnical Geoenviron Eng 2004;130(11):1121–30.
[24] Yegian MK, Catan M. Soil isolation for seismic protection using a smooth synthetic liner. J. Geotechnical Geoenviron Eng 2004;130(11):1131–9.
[25] Tsiavos A, Sextos A, Stavridis A, Dietz M, Dihoru L, Alexander NA. Large-scale experimental investigation of a low-cost PVC 'sand-wich' (PVC-s) seismic isolation for developing countries. Earthquake Spectra 2020;36(4):1886–911.
[26] Tsiavos A, Sextos A, Stavridis A, Dietz M, Dihoru L, Nicholas A. Low-cost hybrid design of masonry structures for developing countries: shaking table tests. Soil Dyn Earthquake Eng 2021;146:106675.
[27] Coulomb CA. Theorie des machines simples, en ayant egard au frottement de leur parties st a la roideur des cordages. Memorie de Mathematique et de Physique de l'Academie Royale 1785;10:161–332.
[28] Tabor D. The mechanism of rolling friction. II. The elastic range. Proc R Soc Lond A 1955;229:198220.
[29] Eldredge KR, Tabor D. The mechanism of rolling friction. I. The plastic range. Proc R Soc Lond A 1955;229:181–98.
[30] Greenwood JA, Minshall H, Tabor D. Hysteresis losses in rolling and sliding friction. Proc R Soc London, Ser A 1961;259(1299):480–507.
[31] Harvey Jr PS, Kelly KC. A review of rolling-type seismic isolation: historical development and future directions. Eng Struct 2016;125:521–31.
[32] Chung LL, Yang CY, Chen HM, Lu LY. Dynamic behavior of nonlinear rolling isolation system. Struct Control Health Monitoring 2009;16:32–54. https://doi.org/10.1002/stc.305.
[33] Tsai MH, Wu SY, Chang KC, Lee GC. Shaking table tests of a scaled bridge model with rolling type seismic isolation bearings. Eng Struct 2007;29(9):694–702.
[34] Harvey Jr PS, Zéhil G-P, Gavin HP. Experimental validation of a simplified model for rolling isolation systems. Earthquake Eng Struct Dyn 2014;43:1067–88.
[35] Cilsalar H, Constantinou MC. Behavior of a spherical deformable rolling seismic isolator for lightweight residential construction. Bull Earthq Eng 2019;17(7):4321–45.
[36] Foti D, Kelly JM. Experimental study of a reduced scale model seismically base isolated with rubber-layer roller bearings (RLRB). Seismic Engineering Monographs, Centro Internacional de Metodos Numericos en Ingenieria, Barcelona, Spain, Monograph. 1996; IS-18. 84-87867-82-0.
[37] Foti D, Catalan Goni A, Vacca S. On the dynamic response of rolling base isolation systems. Struct Control Health Monitoring 2013;20:639–48.
[38] Foti D. Rolling devices for seismic isolation of lightweight structures and equipment. Design and realization of a prototype. Struct Control Health Monitoring 2019;26(3).
[39] Menga N, Bottiglione F, Carbone G. The nonlinear dynamic behavior of a Rubber-Layer Roller Bearing (RLRB) for vibration isolation. J Sound Vib 2019;463:114952. https://doi.org/10.1016/j.jsv.2019.114952.
[40] Taciroglu E, Çelebi M, Ghahari SF, Abazarsa F. An investigation of soil-structure interaction effects observed at the MIT Green Building. Earthquake Spectra 2016;32(4):2425–48.
[41] Mylonakis G, Gazetas G. Seismic soil-structure interaction: beneficial or detrimental? J Earthquake Eng 2000;4(3):277–301.
[42] PEER NGA Strong Motion Database. Pacific Earthquake Engineering Research Center, University of California, Berkeley. https://ngawest2.berkeley.edu/. Accessed 08 October 2018.
[43] Ordonez D, Foti D, Bozzo L. Comparative study on the inelastic structural response of base isolated buildings. Earthquake Eng Struct Dyn 1996;32:151.
[44] Castaldo P, Tubaldi E. Influence of ground motion characteristics on the optimal single concave sliding bearing properties for base-isolated structure. Soil Dyn Earthquake Eng 2018;104:346–64.
[45] Tsiavos A, Mackie KR, Vassiliou MF, Stojadinovic B. Dynamics of inelastic base-isolated structures subjected to recorded ground motions. Bull Earthq Eng 2017;15(4):1807–30.
[46] Tsiavos A, Haladij P, Sextos A, Alexander NA. Analytical investigation of the effect of a deformable sliding layer on the dynamic response of seismically isolated structures. Structures 2020;27:2426–36.
[47] Tsiavos A, Schlatter D, Markic T, Stojadinovic B. Experimental and analytical investigation of the inelastic behavior of structures isolated using friction pendulum bearings. Procedia Eng 2017;199:465–70.
[48] Tsiavos A, Stojadinovic B. Constant yield displacement procedure for seismic evaluation of existing structures. Bull Earthq Eng 2018;17:2137–64.